Effects of Stress Wave Forms on Low Cycle Corrosion Fatigue Strength

AUTHOR(S):

ENDO, Kichiro; KOMAI, Kenjiro

CITATION:

ENDO, Kichiro ...[et al]. Effects of Stress Wave Forms on Low Cycle Corrosion Fatigue Strength. Memoirs of the Faculty of Engineering, Kyoto University 1965, 27(4): 415-432

ISSUE DATE:

1965-12-10

URL:

http://hdl.handle.net/2433/280639

Effects of Stress Wave Forms on Low Cycle Corrosion Fatigue Strength

By

Kichiro ENDO* and Kenjiro KOMAI*

(Received June 30, 1965)

Studies have been made on the influence of trapezoidal stress wave forms on low cycle corrosion fatigue strength. The electrode potential of the specimens has been observed against the saturated calomel electrode during cycles.

The corrosion fatigue strength is much affected by the stress wave forms. The stressless time, the varying stress time and the maximum stress time in one cycle show each effect on the life of specimens, and the deleterious effect of the varying stress time is the most conspicuous. The potential variation during one cycle has close relations with the lives.

1. Introduction

Fatigue strength in corrosive environments is much affected by the stress cycle frequency, and the S-N curve shows no horizontal portion. It is necessary, therefore, to indicate the fixed number of stress cycles and the cycle frequency for the corrosion fatigue strength.

One of the authors explained[1] the effect of cycle frequency by the corrosion effect "k" which was given by the relation between the test time and the ratio of the fatigue strength in air to the one in corrosives, and S-N curves of corrosion fatigue under various test conditions were obtained by using the criterion.

The corrosion effect "k" depends only on testing time in tap water, but it becomes greater at a higher frequency in saline. In usual fatigue tests, however, the stress wave forms being sinusoidal, the time for a given number of cycles together with the stress rates varies according to the cycle frequency. Therefore, it will be impossible to find out if the effect of cycle frequency on the corrosion effect is due to the stress rate or to cycle numbers.

At considerably lower cycle frequencies the corrosion fatigue seems to correlate with the stress corrosion. The stress applied to structures is under

* Department of Mechanical Engineering

considerably lower frequencies than the frequency used in usual corrosion fatigue tests, so that it is doubtful whether or not to apply the criterion mentioned above as it is. The stress wave forms applied to structures, moreover, are similar to trapezoidal, being much different from sinusoidal.

It is known that electrochemical phenomena play important roles in corrosion fatigue. Surface potentials of the test specimen in an electrolyte, therefore, have been studied by many investigators. But these electrode potentials were measured against the cycle numbers of stresses or under static load, and the potential variation during each cycle in fatigue testing has not been referred to. In a low cycle fatigue under large stresses, the potential variation during one cycle is considered to have close relations with the corrosion fatigue strength.

To investigate these problems, a fatigue testing machine was constructed in order that stress rate, maximum stress time and stressless time in trapezoidal stress waves were variable. Studies have been made on the influence of the stress wave forms on low cycle corrosion fatigue strength, observing the electrode potential against the saturated calomel electrode during one cycle and through stress cycles.

2. Testing Methods

A corrosion fatigue testing machine was designed to perform trapezoidal stress wave forms in which stress rate, stressless time and maximum stress time were variable. The machine is shown in Fig. 1. Rotation of motor is changed to straight line motion of constant velocity by a cam ①. The motion magnified by a lever ② drives dead weights ④ on a frame ③ up and down. As a spring ⑤ is located between a free end of cantilever type test piece and the dead weights, a bending moment proportional to the movement of dead weights operates on specimens ⑥ in accordance with the spring constant of the specimen and of the spring, and ten specimens set in a row are subjected to optional stress rates simultaneously. The maximum stress is maintained by dead weights which are detached by lowering the frame, and stressless conditions are given by lifting up the frame enough to make the extension of the spring zero. The maximum stress time, which is the time maintaining the maximum stress constantly, and the stressless time are varied by the combination of brake-motor and micro switch. The cycle frequencies are varied by the period of start and stop of the brake-motor controlled by a time switch. An example of the stress wave forms given by this testing machine is shown in Fig. 2.

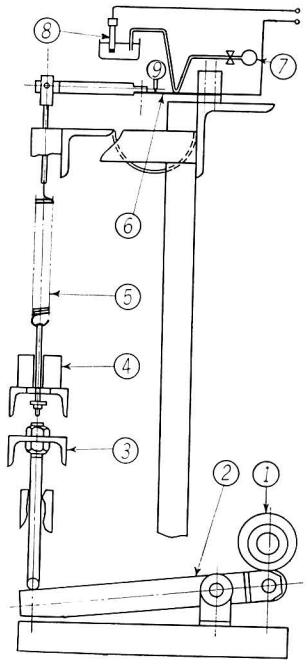

Fig. 1. Schematic diagram of testing machine.

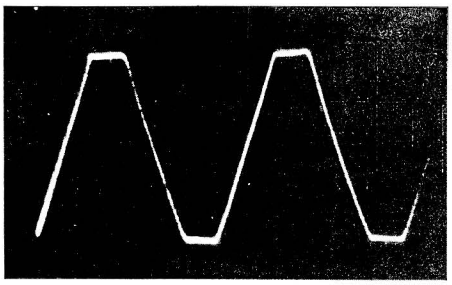

Fig. 2. An example of stress wave forms.

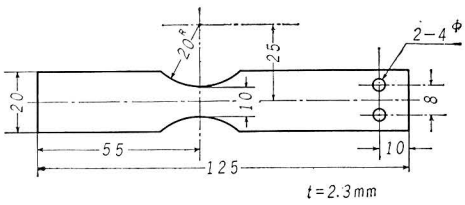

Fig. 3. Dimensions of test specimens.

As a corrosive environment, 1% NaCl aqueous solution was poured on the tension side of the critical section of specimens passing through the flow regulator ⑦.

A capillary tube being located in precisely constant distance over the tension side of the minimum cross section of specimens, the electrode potential was measured against the saturated calomel electrode ⑧. Potential responses resulting from stress variations were recorded on the input balancing type recorder which had a zero adjusting circuit. The sensibility of the recorder is 10 mV on a full scale of 250 mm, and its response rate is 0.08 sec/mV.

The cantilever type test specimen is shown in Fig. 3. The nominal stress is calculated from the stress at the minimum cross section. The strain amplitude of specimens is recorded continuously on a pen writing oscillograph by differential transformers. The zero point and the degree of amplification are calibrated by dial gauges ⑨.

3. Effects of Stress Rate

3.1. Stress wave forms and materials tasted

Patterns of stress wave forms are shown in Fig. 4. In the first group (a),

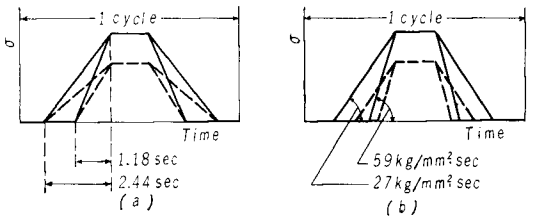

Fig. 4. Patterns of stress wave forms.

the varying stress time, time from zero stress to maximum stress, is kept constant, 1.18 sec and 2.44 sec. In the second group (b), the stress rate is kept constant, 27 kg/mm²·sec and 59 kg/mm²·sec. In either group of tests, the value of maximum stresses is varied, the maximum stress time being constant, 1.2 sec. Accordingly, the stress rate becomes greater at a higher stress in the group (a) and the varying stress time becomes longer at a higher stress in the group (b). The stress cycle frequency is 8.2 cpm, time of one cycle being 7.3 sec.

The test material is a high carbon steel whose chemical composition is shown in Table 1. The material is quenched in oil from 850°C, and is tempered at 550°C for 1 hour. Its mechanical properties are shown in Table 2.

Table 1. Chemical composition of test material (%).

	C	Si	Mn	P	S	Ni	Cr	Mo	Cu
SK 4	0.90	0.29	0.92	0.014	0.011	0.06	0.21	0.04	0.13

Table 2. Mechanical properties of specimens.

Yield point σ_S (kg/mm²)	Ultimate strength σ_B (kg/mm²)	Elongation φ (%)	Reduction of area ψ (%)
90	112	14	30

3.2. Results and discussions

The fatigue tests are repetitions of pulsating bending stresses. The relation between the increment of strain amplitude and the number of cycles is shown in Fig. 5 schematically. *Ni* denotes number of cycles before crack initiation, in which the increment of strain amplitude is contributed to by pits formation. The strain amplitude shows steep increases after *Ni*, which are caused by the decrease of cross section and stress concentration due to the initiation and propagation of

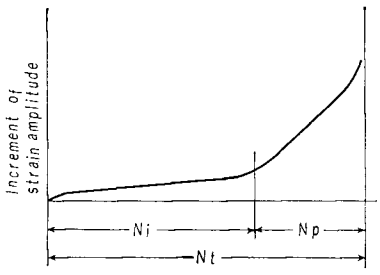

Fig. 5. Schematic diagram of increment of strain amplitude *vs.* number of cycles.

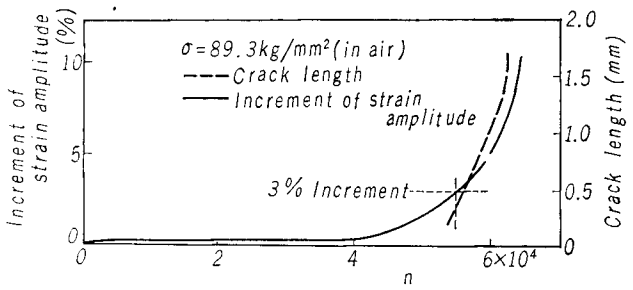

Fig. 6. Relation between crack length and increment of strain amplitude for specimens tested in air.

cracks. The final failure takes place when this increment exceeds a value. Relations between the crack length and the increment of strain amplitude for a specimen tested in air are shown in Fig. 6. Crack length of 0.3 mm is detected at 3% increment of strain amplitude; thereafter the fatigue crack propagates corresponding with the increment of strain amplitude.

In corrosive environments fine cracks are difficult to detect owing to pits formation. Hence considering the sensibility of measuring instruments, 3% increment of strain amplitude was tentatively regarded as crack initiation point. It was made certain from microscopic observations of corrosion fatigue specimens that cracks were not found at 3% increment because of the pits formed from hair cracks, but that many fine cracks were detectable at 6% increment. From above results it was decided that crack propagation period Np was consisted of the cycle numbers from 3% increment of strain amplitude to final failure. Therefore, the total number of cycles to failure Nt is expressed as $Nt=Ni+Np$.

A S-N diagram which is the relation between maximum stress and Nt is shown in Fig. 7, containing the test results in air. The relation based on Np

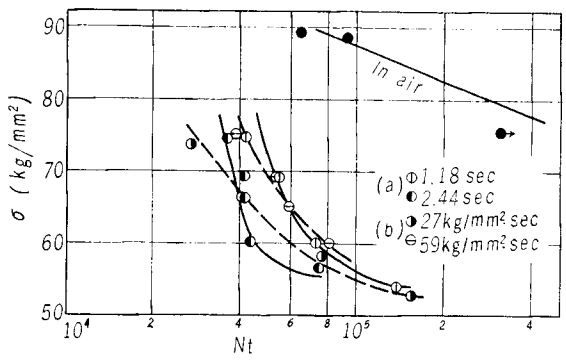

Fig. 7. Maximum stress *vs.* number of cycles to failure Nt.

is shown in Fig. 8. In the figures, solid lines show the group (a) where the parameter is the varying stress time, and dotted lines show the group (b) of the parameter of the stress rate.

The life Nt gets cut short by the longer varying stress time or the smaller stress rate. Though crack propagation period Np is much smaller than Nt, similar relations are found in Fig. 8.

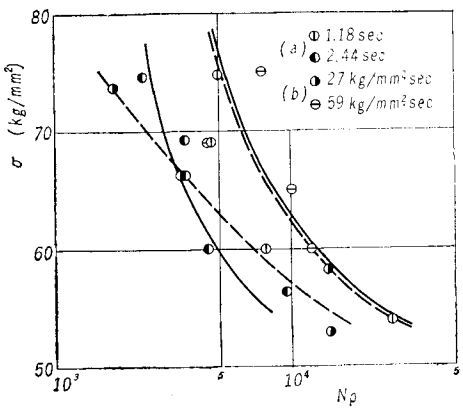

Fig. 8. Maximum stress *vs.* number of cycles in crack propagation period Np.

The relation between $\Delta Np/\Delta Nt$ and the maximum stress is shown in Fig. 9. ΔNt and ΔNp denote the difference of cycle numbers in Np and in Nt respectively when the varying stress time is varied. The ratio $\Delta Np/\Delta Nt$ is smaller at a higher stress. Since the effect of stresses is greater than that of corrosion at a higher stress, test specimens are rapidly broken down owing to the fast crack propagation when pits reach a given density. This fact shows that the varying stress time has its effect on the crack initiation and crack propagation period at a lower stress, while the effect on the latter is smaller than that on the former at a higher stress range.

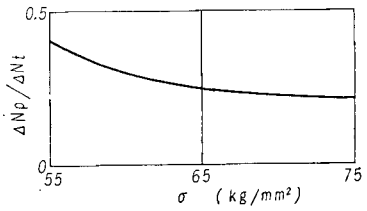

Fig. 9. Ratio of the variation of the crack propagation period ΔNp to the variation of the total life ΔNt according to the varying stress time *vs.* maximum stress.

3.3. Electrode potential

When metals are immersed in an electrolyte, coarse portions on oxide films of specimens that contain cracks or flaws penetrating the film to base metals are anodic while sound portions are cathodic. These construct local cells. Gough's criterion is as follows[2)3)]; "Increased velocity of corrosion under corrosion fatigue conditions is due to the effect of cyclic strains on the porosity and rupture of protective films, and the protective films are distinctly weakened on slip lines of specimen surfaces. Further the corrosion works upon slip lines preferentially under slip motions and does not work on slip lines which have generated before the corrosion attack." Thus, when an electrolyte

is a good conductor, equilibrium potentials are detected as corrosion potentials.

The potential variation in corrosion fatigue has been measured by some investigators. Rjabchenkov[4] found that potentials of specimens were shifted to anodic under pulsating tension more than under pulsating compression. Spähn[5] showed that potential variation during life of specimens was divided into three stages and that stress cycle frequencies had the effect on the first stage where potential variation was decreased with increased cycle frequencies. These variations of electrode potential, however, were against cycle numbers of stresses, and the relation between the potential variation during each cycle and stress wave forms hasn't been referred. It may be the stress wave form that affects the corrosion fatigue strength, because the corrosion damage is regarded as the accumulation of potential variation during each cycle.

A polarization curve of local cells is shown in Fig. 10, where i_a and i_c denote currents of local anode and local cathode respectively. Cathode polarization curve C is regarded independent to the value of stresses. As A_0 and A_m show anode polarization curve under a zero stress and under a maximum stress respectively, e_0 and e_m are the equilibrium potentials under a zero stress and under a maximum stress respectively. The activity variation of steels due to stresses is so small that its effect is able to be neglected. i_{a0} and i_{c0} are local anode and local cathode currents under zero stresses. i_{am} and i_{cm} are local anode and local cathode currents under maximum stresses. e_0 is more cathodic than e_m, so i_{a0} is smaller than i_{am}. The movement of local anode polarization curve due to the plastic slip, however, is retarded to the change of stresses to some extent. The mixed potential does not instantly shift to the equilibrium potential which satisfies the condition of $|i_{am}| = |i_{cm}|$, so that the mixed potential e_m' has the value of $e_m < e_m' < e_0$ at an instant when the local anode polarization curve has become A_m. e_m' gradually reaches the more anodic equilibrium potential e_m after the maximum stress is maintained for some time. When the stress is reduced, the potential recovers in retard of the stress variation in the same way. Thus the potential during one cycle may be affected by stress wave forms.

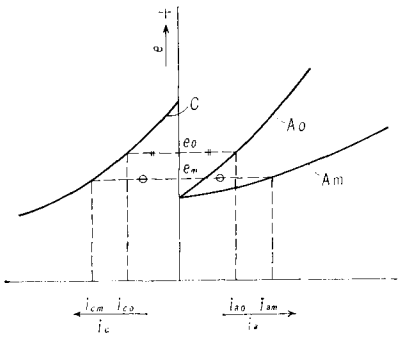

Fig. 10. Schematic diagram of polarization curve of local cell.

Fig. 11 shows the potential variation during one cycle measured at various cycle numbers in fatigue tests under the wave form where the varying

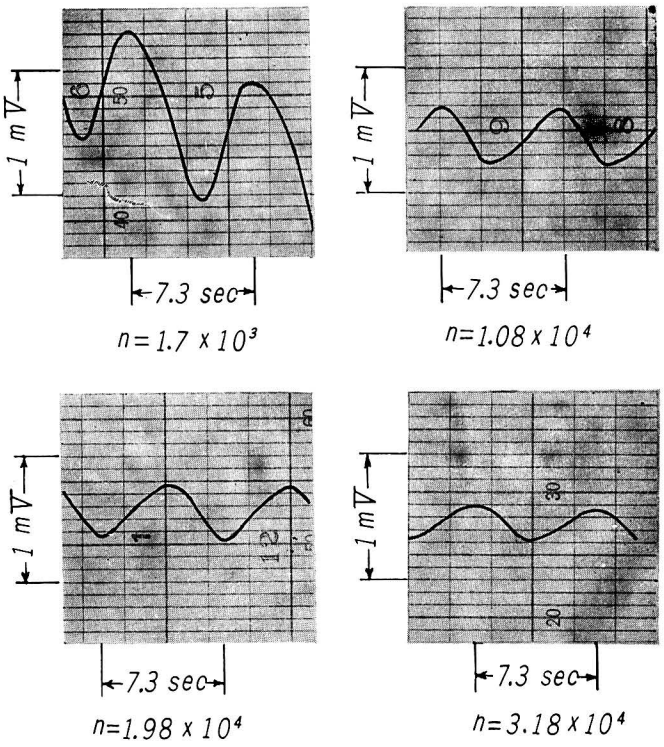

Fig. 11. Potential variation at various stress cycles. Varying stress time 1.18 sec, maximum stress 74.6 kg/mm².

stress time is 1.18 sec. The amplitude of potential and its deviation to the anodic direction are greater at the beginning of stress cycles, and these decrease with the progress of cycles. Potential variations become sinusoidal, though stress wave forms are trapezoidal. The potentials are collated in Fig. 12 and Fig. 13 with the stress wave forms. Fig. 12 is the case where the

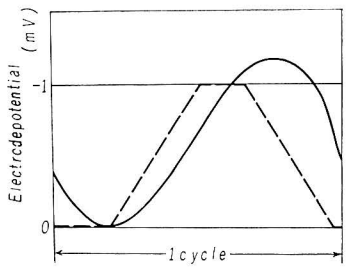

Fig. 12. Variation of electrode potential (solid line) and stress (dotted line) during one cycle. Varying stress time 2.44 sec.

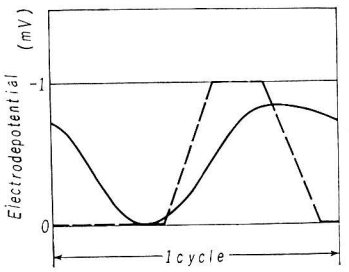

Fig. 13. Variation of electrode potential (solid line) and stress (dotted line) during one cycle. Varying stress time 1.18 sec.

varying stress time is 2.44 sec (the stress rate is 27 kg/mm²·sec), and Fig. 13 is 1.18 sec (the stress rate is 55.5 kg/mm²·sec), and the maximum stress is 65.6 kg/mm² and the cycle number is 2×10^3 in both of the figures. Since the corrosion potential of specimens is retarded to the change of stress, the potential follows up the stress better and is more anodic at a smaller stress rate. As mixed potentials of the stress wave forms in Fig. 12 and Fig. 13 do not reach the equilibrium potentials, the corrosion fatigue strength is considered to be affected by not only the varying stress time but also the maximum stress time and the stressless time in one cycle. The evidence is also presumed from Fig. 7. When the stress rate is small, the life is shorter owing to the prolongation of the varying stress time under higher cyclic stresses, but the difference of lives caused by the variation of the stress rate becomes smaller under lower cyclic stresses. Though the fraction of the varying stress time to the total cycle time is smaller under lower cyclic stresses as is shown in Fig. 4(b), the maximum stress time is unvaried, and the maximum stress time becomes more effective than the varying stress time on lives. The effect of the stressless time and the maximum stress time will be further investigated in the next chapter.

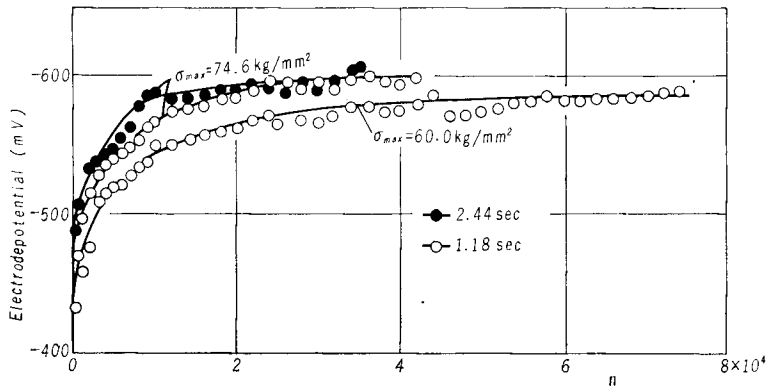

Fig. 14. Potential variation through stress cycles against saturated calomel electrode.

The potential through stress cycles is shown in Fig. 14. The potential is more anodic at a higher stress and tends to anodic at a longer varying stress time under the same stress, in accordance with the tendency of the potential during one cycle. Rjabchenkov[4] showed that the potential was more anodic at lower cycle frequencies after a given number of cycles in sinusoidal stress wave forms. These and the present test results on the potential variation during one cycle mean that it is not the cycle number of stresses but the stress rate that makes the electrode potential anodic.

4. Effects of Stressless Time, Maximum Stress Time and Cycle Frequency

4.1. Stress wave forms and materials tested

Stress wave forms are shown in Fig. 15. The frequency is 8.2 cpm in the wave form A, one cycle being equal to 7.3 sec. In the wave form B test specimens are subjected to stresses of the same wave form as A once in every 45 sec, the remaining time being maintained by zero stresses. Contrary to the wave form B, in the wave form C, the load of specimens is removed once in every 45 sec, the remaining time being maintained by the maximum stresses. In the wave form D, the stressless time t_0, the varying stress time t_a and the maximum stress time t_m in the wave form A being prolonged, one cycle is equal to 45 sec. In all the wave forms of B, C and D the frequency is 1.3 cpm. The total cycle time is expressed as $t=t_0+2t_a+t_m$.

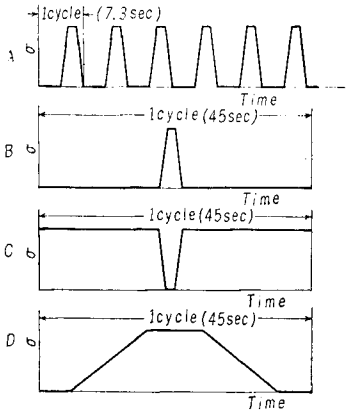

Fig. 15. Patterns of stress wave forms.

The chemical composition of the material tested is shown in Table 3. The material is quenched in water from 480°C, and is tempered at 120°C for

Table 3. Chemical composition of test material (%).

Zn	Mg	Cu	Si	Fe	Mn	Ti	Cr	Al
5.42	2.47	1.66	0.07	0.15	0.01	0.02	0.01	bal

24 hours. Though mechanical properties are improved by the treatments, corrosion resistances are deteriorated. Being different from common alloy 75S (extra super duralumin), this material is made sensitive to stress corrosion because of scarce contents of Cr. Mechanical properties of specimens after heat treatments are shown in Table 4.

Table 4. Mechanical properties of specimens.

Yield strength $\sigma_{0.2}$ (kg/mm²)	Ultimate strength σ_B (kg/mm²)	Elongation φ (%)
32.0	36.6	8

4.2. Results and discussions

The *S-N* diagram where *Nt* is plotted against maximum stresses is shown

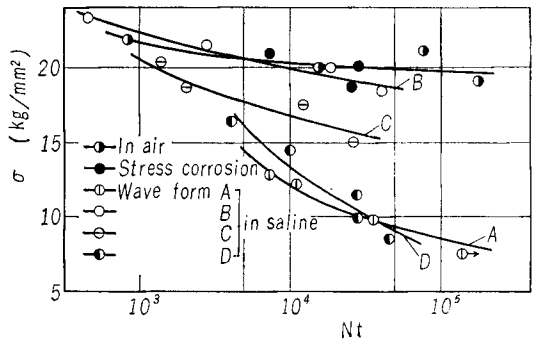

Fig. 16. Maximum stress *vs.* number of cycles to failure *Nt*.

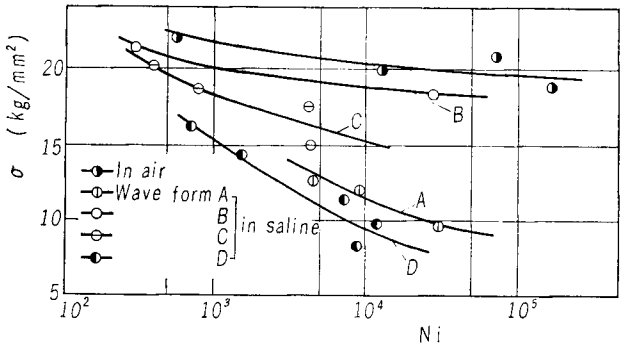

Fig. 17. Maximum stress *vs.* number of cycles in crack initiation period *Ni*.

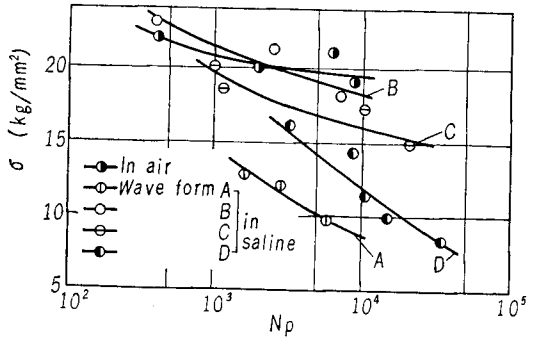

Fig. 18. Maximum stress *vs.* number of cycles in crack propagation period *Np*.

in Fig. 16. Test results in air are obtained under the stress wave form A. The relations between the maximum stress and the crack initiation period *Ni* and between the maximum stress and the crack propagation period *Np* are shown in Fig. 17 and Fig. 18 respectively.

1) Effects of corrosive environments — The specimen tested in saline under the stress wave form B has the same strength as the one tested in air, as is shown in Fig. 16. Relations between the increment of strain amplitude and the number of cycles for specimens tested in air and in saline are shown in Fig. 19, where (i), (ii) and (iii) are the results under the wave form B (in saline), the wave form A (in saline) and the wave form A (in air) respectively. The increment of strain amplitude tested in air increases rapidly after considerable cycles following final failure, so the ratio of *Np* to *Nt* is small. On the other hand the increment in saline under the wave form B increases from a fairly early stage of stress cycles and its increasing rate is low, and the ratio of *Np* to *Nt* is great. Consequently the rate of crack propagation is smaller in corrosive environments than in air. The crack initiation period *Ni* is, however, decreased by the intergranular corrosion or the surface roughening under corrosion. These bear analogy to the relation between smooth specimens and notched specimens.

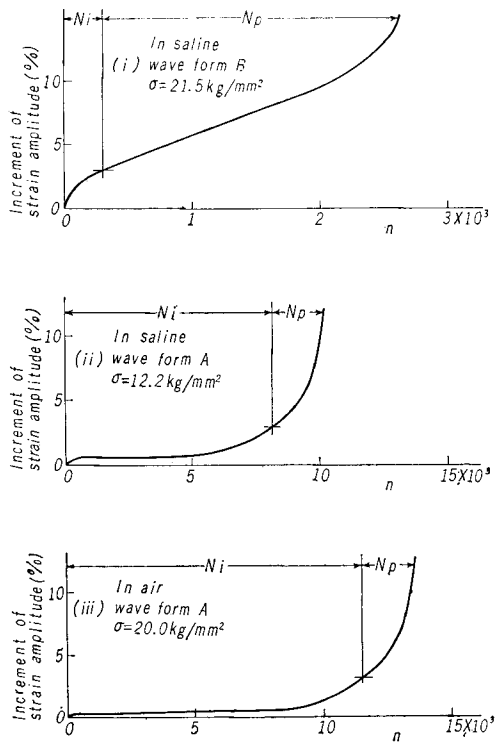

Fig. 19. Increment of strain amplitude through stress cycles.

2) Stress corrosion and corrosion fatigue — Test results of stress corrosion are inserted in Fig. 16. Life times under the stress corrosion are converted into cycle numbers at the rate of 45 sec per cycle which is equal to the cycle time of the wave form B, C and D. Protective films being destroyed by the action of varying stresses, the damage in corrosion fatigue has been found generally more than in stress corrosion. In the present test too, the corrosion

fatigue strength under the wave form C, whose cycle time almost consists of the maximum stress time, is smaller than the strength under the stress corrosion as well as under the wave form A, and the damage of the varying stress time is proved. Wasserman[6] showed in bending stress corrosion tests of similar aluminum alloy, that the life under constant stresses was longer than the life under stresses reversed at every two hours. On the other hand the corrosion fatigue strength under the wave form B, whose cycle time almost equals the stressless time, is close to the strength under the stress corrosion. Consequently the damage caused by varying stresses is reduced by the stressless corrosion.

3) Effects of stressless time — The stress wave form B whose cycle time is 45 sec is derived from prolongation of the stressless time t_0 in the wave form A. As is shown in Fig. 16, the fatigue strength under the wave form B is much greater than that under the wave form A. The number of cycles to failure increases when the cycle time is lengthened by the increase of t_0. The stressless time in this case, therefore, has protective effects which decrease the corrosion fatigue damage. The effect is recognized in both the crack initiation and the crack propagation as is found in Fig. 17 and Fig. 18. The comparison between the strength at 10^4 cycles in *Ni* and the strength at 10^4 cycles in *Np* is shown in Table 5, together with the ratio of the strength under the wave form B, C and D to the strength under the wave form A. The protective effect due to the stressless corrosion in N_p is quite greater than that in *Ni*.

Table 5. Comparison between strength at cycle numbers 10^4 in *Ni* and strength at cycle numbers 10^4 in *Np* for stress wave form A, B, C and D.

stress wave form	A (kg/mm²)	B (kg/mm²)	B/A	C (kg/mm²)	C/A	D (kg/mm²)	D/A
Ni	11.3	18.8	1.7	15.2	1.3	9.5	0.84
Np	8.7	18.1	2.1	15.9	1.8	11.9	1.3

4) Effects of maximum stress time — The stress wave form C whose cycle time is 45 sec is derived from prolongation of the maximum stress time t_m in the wave form A. As is shown in Fig. 16, number of cycles to failure increases when the frequency is lowered by the increase of t_m. Therefore, t_m has the protective effect as well, which is more effective in *Np* than in *Ni*. The strength under the wave form C, however, is smaller than that under the wave form B, and the destructive effect of the maximum stress time t_m which increases the damage of corrosion fatigue is greater than that of t_0

when the cycle time t is constant. This is a matter of course, because the wave form B is a combination of stressless corrosion and corrosion fatigue while the wave form C is a combination of stress corrosion and corrosion fatigue.

5) Effects of cycle frequency — The stress wave form D whose cycle time is 45 sec is derived from prolongation of t_0, t_a and t_m in the wave form A. Though the maximum stress time is longer compared to the wave form A, the varying stress time is also longer, and the fatigue strength is lowered remarkably as is shown in Fig. 16. The destructive effect of the varying stress time is greater on *Ni* than on *Np* as was mentioned at the previous chapter. Therefore, the destructive effect owing to the prolongation of t_a in the wave form D being greater in *Ni*, the curve of the wave form D is lower than the one of the wave form A in Fig. 17. On the other hand the protective effect of t_m and t_0 on *Np* grows stronger than the destructive effect of t_a on *Np*, so the curve of the wave form D is higher than the one of the wave form A in Fig. 18. The ratio of the strength under the wave form D to the strength under the wave form A is shown in Table 5. The curve of the wave form D intersects the one of the wave form A in Fig. 16 owing to this interdependence. The results are summarized in Table 6. + sign means

Table 6. Effects of stressless time (t_0), varying stress time (t_a) and maximum stress time (t_m) during one cycle on the cycle numbers of *Ni*, *Np* and *Nt*. + sign means protective effects and − sign means destructive effects.

	When t is increased by t_0, t_a and t_m.			When t is constant.		
	t_0	t_a	t_m	t_0	t_a	t_m
Ni	+	−	+	+	−	−
Np	+	−	+	+	−	−
Nt	+	−	+	+	−	−

protective effects and − sign means destructive effects. When a cycle frequency is lowered according to the increase of t_a, the destructive effect of t_a appears in *Ni*, *Np* and *Nt*. When a cycle frequency is decreased by the increase of t_0 or t_m, protective effects appear, the effect of t_0 being greater than that of t_m. When a cycle frequency is constant, t_a and t_m have destructive effects in *Ni*, *Np* and *Nt*, the effect of t_a being greater than that of t_m. It may be concluded that the smaller number of cycles to failure at lower frequencies under usual corrosion fatigue of sinusoidal wave form is due to the longer varying stress time rather than the greater time for corrosion.

4.3. Cracks

Since corrosive agents work selectively on grain boundries of high strength aluminum alloy 75S, intercrystalline cracks are found in specimens subjected to the corrosion fatigue in saline as is shown in Fig. 20 (a). Whilst specimens

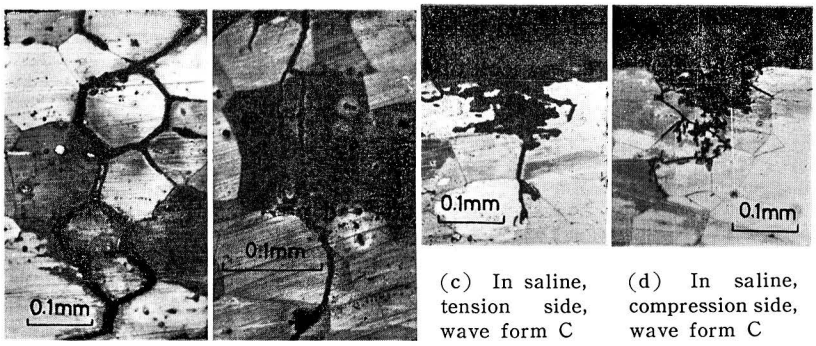

(a) In saline (b) In air (c) In saline, tension side, wave form C (d) In saline, compression side, wave form C

Fig. 20. Fatigue cracks of test specimens.

tested in air have transcrystalline cracks as Fig. 20 (b). Intercrystalline cracks under the stress corrosion show considerable branching or thickening of crack tips. Though cracks appear only in the tension side of specimens under the stress corrosion, cracks are also found in the compression side of specimens under the corrosion fatigue of pulsationg bending, as is shown in Fig. 20 (c) and (d). Cracks are longer in the tension side than in the compression side, and the branching, the thickening and the pits formation of cracks are conspicuous in the latter, especially in the wave form B and C. Though the damage due to compressive stresses is known to be much smaller than that due to tensile stresses in usual cycle frequencies, it was reported that compressive stresses gave considerable damages to specimens under stress corrosion of reversed tension and compression[6]. Therefore, compressive stresses are known not to be negligible in low cycle corrosion fatigue.

From the observations, protective effects of t_0 and t_m in Np are considered due to the decrease of crack propagation rate caused by the lowering of stress concentration according to the branching, the thickening and the pits formation of cracks. The decrease of propagation rate is presumed from the comparison of the increments of strain amplitude between the wave form A and B which are shown in Fig. 19.

4.4. Electrode potential

The potential during one cycle is collated in Fig. 21 with the stress wave

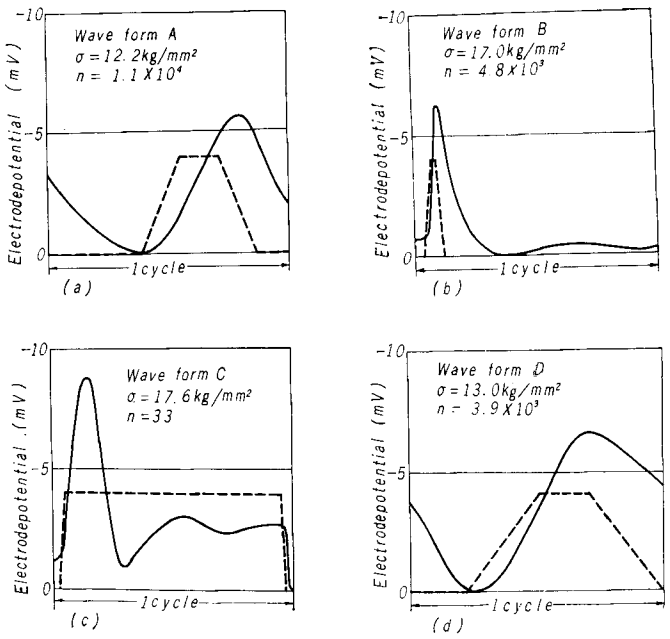

Fig. 21. Variation of electrode potential (solid line) and stress (dotted line) during one cycle.

form A, B, C and D. Solid lines show the electrode potential and dotted lines show the stress. The potential of the wave form B tends to cathodic in retard of unloading and thereafter the potential is maintained in the stressless time. The potential of the wave form C is the most anodic after a stress becomes the maximum value, but afterwards the potential becomes somewhat cathodic owing to the repair of oxide films. Compared with the wave form B, however, the recovery is imperfect, and the life under the wave form C is shorter than that under the wave form B owing to the difference of dissolution rate. The dissolution rate is the highest in the wave form D whose varying stress time is the longest among these wave forms. Therefore, the damage under the wave form D is the most intense, especially in *Ni*. From these evidences the protective effects of t_0 and t_m in *Ni* are considered due to the recovery of corrosion potentials during the times.

The potential against the saturated calomel electrode is −780 mV, being constant through stress cycles. Different tendencies are found in the alminum alloy from those of the steel.

Nobe and Tan[7] found that potential responses depended upon the character of semiconductor of oxide films, the sensibility of metals to corrosions and the strength of metals, and that the potential of steel became anodic through

stress cycles though the potential of brass and silver was unvariable. It may be due to the difference of oxide films that the dependence of potentials on stress cycles is different between the steel and the aluminum alloy in the present tests.

5. Corrosion Effect "k"

One of the authors explained the effect of cycle frequency on the fatigue strength by the corrosion effect "k". The corrosion fatigue strength σ_c is expressed as $\sigma_c k=\sigma_{(N)}$, where $\sigma_{(N)}$ denotes the fatigue strength in air at the cycle number of N. "k" is given by $k=1+a\cdot\log(bc^{f}t+1)$. As $\sigma_{(N)}$ is a function of N alone and "k" depends mainly on time t, the corrosion fatigue strength at a given number of cycles is smaller at lower frequencies since the time for corrosion is greater. On the other hand, the corrosion fatigue strength is smaller at longer varying stress time in trapezoidal stress wave forms. When the decrease of cycle numbers to failure at lower frequencies in sinusoidal wave forms is considered due to the increase of the varying stress time, the increase of the corrosion effect "k" at lower frequencies must be due to the longer varying stress time. Therefore, the variation of "k" may not be due to the corrosion time, but must be due to the varying stress time. In the present tests, the corrosion effect "k" diminishes on the contrary under lower frequencies in the case of the wave form B and C. These are contributed to by the increase of t_0 and t_m.

6. Conclusions

Studies have been made on the effect of stress wave forms on the low cycle corrosion fatigue strength under trapezoidal stresses to make clear the mechanism of corrosion fatigue and to make some contributions to the strength of structural members. The fatigue tests were carried out with a carbon steel and an aluminum alloy. The following things are made clear;

1) The corrosion fatigue strength is affected by the stress wave forms. The life gets cut short by the longer varying stress time in one cycle or the lower stress rate, because the corrosion potential of the specimens is retarded to and does not follow up the stress. The varying stress time has its effect on the period of crack initiation and of crack propagation.

2) When cycle frequency is constant, the varying stress time (t_a) and the maximum stress time (t_m) have destructive effects which increase corrosion fatigue damages, especially in the crack initiation period Ni. The effect of t_a is greater than that of t_m, being due to the difference of recovery of

the corrosion potential.

3) When cycle frequency gets low according to the increase of the varying stress time, destructive effects appear. When cycle frequency gets low by the increase of the stressless time (t_0) or the maximum stress time (t_m), protective effects, which decrease corrosion fatigue damages, appear. The protective effects are due to the recovery of the corrosion potential in the crack initiation period. In the crack propagation period the effects are due to the decrease of crack propagation rate caused by the lowering of stress concentration according to the branching, the thickening and the pits formation of cracks.

4) The corrosion potential of the specimens is more anodic at a longer varying stress time or at a lower stress rate because of the following-up of the potential to the stress. The anodic potential recovers to some extent during the stressless time or the maximum stress time in the wave form B and C.

5) The potential of the steel through stress cycles is more anodic at a higher stress, and tends to anodic at a longer varying stress time in accordance with the potential during one cycle. But in the aluminum alloy, the potential against the saturated calomel electrode is −780 mV, being constant through stress cycles.

References

1) K. Endo and Y. Miyao; Proc. 1st Japan Cong. on Testing Materials p. 17, (1958).
2) H. J. Gough; J. Inst. of Metals, **49**, p. 17 (1932).
3) H. J. Gough and D. G. Sopwith; Proc. Roy. Soc. (London) **135A**, p. 392 (1932).
4) A. V. Rjabchenkov; by courtesy of H. Spähn, Ref. 5).
5) H. Spähn; Metalloberfläche, **16**, p. 299 (1962).
6) G. Wasserman; Z. Metallkde., **34**, p. 297 (1942).
7) K. Nobe and S. Tan; Corrosion, **18**, p. 391 (1962).